Multi-criteria protection scheme for online element failure detection in shunt capacitor banks

Goodarzi, Ali; Allahbakhshi, Mehdi ; Tajdinian, Mohsen ; Popov, Marjan

DOI
10.1049/iet-gtd.2020.0347

Publication date
2020

Document Version
Final published version

Published in
IET Generation, Transmission and Distribution

IET Generation, Transmission & Distribution

Research Article

IET Journals
The Institution of Engineering and Technology

Multi-criteria protection scheme for online element failure detection in shunt capacitor banks

ISSN 1751-8687
Received on 24th February 2020
Revised 2nd June 2020
Accepted on 16th June 2020
E-First on 9th July 2020
doi: 10.1049/iet-gtd.2020.0347
www.ietdl.org

Ali Goodarzi[1], Mehdi Allahbakhshi[1] ✉, Mohsen Tajdinian[1], Marjan Popov[2]

[1]*School of Electrical and Computer Engineering, Shiraz University, Shiraz, Iran*
[2]*Delft University of Technology, Faculty of EEMCS, Mekelweg 4, 2628 CD, Delft, The Netherlands*
✉ *E-mail: allahbakhshi@shirazu.ac.ir*

Abstract: This paper deals with a fault detection investigation of SCBs, and it is focused on the faulty phase detection and the number of faulty capacitor units. Unlike previous methods, the proposed method provides a relay decision making criterion which determine the faulty capacitors, and the number of capacitor failures in case of multiple faulty phase conditions. The proposed algorithm is applied on different wye configurations of SCBs considering different protection designs (i.e., fuseless, internally and externally fused units). Since the detection of capacitor failures in SCBs are based on the fundamental phasor component, there may occur a significant delay in decision making in the case of an external short circuit fault in the power system. The aforementioned condition, which will be mathematically proven, happens due to a capacitor discharge after fault clearance. To deal with this condition, a method is proposed by applying an algorithm, in which the fundamental component of the voltage signal is extracted in one cycle. Performance evaluations associated with the proposed method are provided for different fault conditions, fault locations, and different levels of harmonics and, they are further discussed through the implementation of the proposed method in MATLAB environment.

1 Introduction

Capacitor units, which are widely employed in power system high-voltage applications, are designed by utilising different fuse-based protection technologies, which can be externally fused, internally fused, or even fuseless. It has been reported that the internally fused and fuseless technologies attract more interest for substation applications as a result of providing appropriate reliability and also fewer cost issues regarding the life cycle [1, 2]. Compared to the externally fused technology of capacitor units, fuseless and internally fused technologies have higher accessibilities. However, the last two technologies confront the disadvantage of having problems in identifying failed units due to a lack of external fuses. As discussed in [3], system imbalance has become a major occurrence in power systems, and as a result, protection and control systems provided for shunt capacitor banks (SCBs) require enhanced algorithms that are able to detect the faulty phases and units of SCBs. The aforementioned enhanced algorithms will help in faster localisation of the faulty phases and units and thus, making the repair and preparation procedure of the SCBs for operation quicker. Also, these algorithms can be helpful for condition monitoring of the SCB capacitor units and consequently can result in the reduction of unscheduled outages of SCBs. It must be mentioned that except for some protection schemes that employ per-phase measurements [1, 4–6], the conventional unbalance protection functions confront challenges regarding localisation of faulty points in SCBs, due to lack of an adequate number of available measurements [7].

By investigation of previously published papers regarding SCBs fault detection, location, and online monitoring focusing on unbalanced protection schemes, it is found that very few research studies have been conducted in this area. Generally, previously published methods are grouped into two categories. The first group of methods is designed for double wye configuration of SCBs and perform its calculations based on the current measured at the neutral point [8–11]. These methods can detect the faulty phase and also the number of failed capacitor units using current-base unbalance relaying. A comprehensive review regarding unbalance protection schemes of double-wye SCBs can be found in [9].

The second group, which is the main interest of this study, concentrates on the single wye configuration of SCBs and is based on the voltage of the neutral point [12–14]. As mentioned in [15], the calculations of these methods are conducted based on the reference of the phase angle of the neutral point from the phase angle of the positive sequence bus voltage. Through this selection of reference angle, the effects of negative sequence voltages on the phase angles of the phase voltages are disregarded. In [16], a method based on the negative sequence current has been proposed for the fault location in the single wye SCB configuration that solves the aforementioned problem regarding negligence of the contribution of the negative sequence in the referenced phase angle. The most recent protection scheme has been proposed in [7], which is based on superimposed reactance (SR). The application of the SR method is done by utilising available voltages for an unbalance protection relay.

It should be noted that through surveying the literature, it is indicated that the research publications mostly focus on the application of the SCBs for the power quality improvement, reactive power management, and voltage stability improvement of the power system through optimal allocation of SCBs in the planning stage [17–22].

By considering the criteria given in [7], even though the SR method seems very comprehensive, some issues have neither been investigated nor addressed. These issues are mainly related to the performance of the protection scheme in case of multiple faulty units at the same time in different phases, the impact of the power system transient faults on the delay time of the relay operation and the impact of harmonic pollution.

This study presents an enhanced indicator for element failure detection that essentially calculates the per unit variations of the capacitor. The presented method, which is applied for each phase separately, utilises only the available voltages of the unbalance protection relay. Similar to [7], the proposed method utilises the fundamental phasor components for the determination of the fault location, without making use of the reference phase angle. The contributions of the study are as follows:

- In addition to fault location identification, the proposed method utilises some uncomplicated calculations to detect and determine

the number of faulty units, as well. The criterion provided by the proposed method, contrary to [7], is also capable of detecting and determining the number of faulty units. The latter criterion is reflected in the newly developed calibrating factors, which are based on the new definition of *k*-factors and the unbalance relay input voltages. The new calibrating factors are able to discriminate the capacitor units' failures that may simultaneously or with sub-cycle delays occur by phase.

- The proposed algorithm, being developed considering different SCB wye configurations, can greatly ease the monitoring of the capacitor units, regardless of the protection design (i.e. fuseless, internally, and externally fused units).
- The other concerns regarding the capacitor failure detection in the SCBs comprise the issue that the numerical protection calculations are usually based on the fundamental phasor component. As a result, significant delays in decision making may occur in case of an external short circuit fault in the power system. In this study, firstly, the behaviour of the SCBs is investigated during a fault. Thereafter, to deal with the impact of the capacitor discharge behaviour of the SCBs after fault clearance on the SCBs' protection scheme, the proposed protection scheme is provided a developed algorithm, in which the fundamental component of the voltage signal is extracted in one cycle. This extra algorithm helps to prevent the undesired delay time in the relay trip signal of the SCBs.

The rest of the paper is organised as follows: the proposed methods and fundamental formulations are discussed in Section 2. Section 3 presents the implementation procedure of the proposed method. Performance evaluation and meaningful conclusions are given in Sections 4 and 5, respectively.

2 Problem statement and proposed algorithm

As previously discussed, the unbalanced protection scheme is the most important and vital protection of the SCBs against internal faults. In the following, the proposed protection scheme for identifying the faulty phase(s) and determining the number of failed units is presented for different SCB configurations. Different SCB configurations as illustrated in Fig. 1, are adopted from IEEE Std C37.99 [23]. It should be noted that the proposed algorithm is generally based on the fundamental phasor component of the neutral point voltage. As a result, the computation of the fundamental phasor component is realised by applying the full-cycle discrete Fourier transform (DFT).

2.1 Calculation of k-factors

Fig. 1*a* shows the SCB configuration with an ungrounded wye connection (Con1). V_N, $V_{A,B,C}$, and $C_{A,B,C}$ correspond to the neutral point voltage, phase to ground voltages regarding each phase, and the capacitor regarding each phase, respectively. Assuming the steady-state condition, by applying Kirchhoff's current law at the neutral point, the following is concluded:

$$\frac{V_{\mathrm{N}}-V_A}{\frac{-\mathrm{j}}{\omega C_A}}+\frac{V_{\mathrm{N}}-V_B}{\frac{-\mathrm{j}}{\omega C_B}}+\frac{V_{\mathrm{N}}-V_C}{\frac{-\mathrm{j}}{\omega C_{\mathrm{C}}}}=0 \Rightarrow (C_A+C_B+C_C)V_{\mathrm{N}}=C_AV_A+C_BV_B+C_CV_C \tag{1}$$

Two *k*-factors are defined as follows:

$$K_A \triangleq \frac{C_A}{C_C} \tag{2a}$$

$$K_B \triangleq \frac{C_B}{C_C} \tag{2b}$$

According to (2), expression (1) can be rewritten as follows:

$$(1+K_A+K_B)V_{\mathrm{N}}=K_AV_A+K_BV_B+V_C \tag{3}$$

By transforming (3) into a matrix form, the *k*-factors can be expressed as follows:

$$\begin{bmatrix}K_A\\K_B\end{bmatrix}=\begin{bmatrix}V_A^{\mathrm{re}}-V_{\mathrm{N}}^{\mathrm{re}} & V_B^{\mathrm{re}}-V_{\mathrm{N}}^{\mathrm{re}}\\ V_A^{\mathrm{im}}-V_{\mathrm{N}}^{\mathrm{im}} & V_B^{\mathrm{im}}-V_{\mathrm{N}}^{\mathrm{im}}\end{bmatrix}^{-1}\begin{bmatrix}V_{\mathrm{N}}^{\mathrm{re}}-V_C^{\mathrm{re}}\\ V_{\mathrm{N}}^{\mathrm{im}}-V_C^{\mathrm{im}}\end{bmatrix} \tag{4}$$

where superscripts re and im correspond to the real and imaginary parts of the voltage phasor component.

The *k*-factors for ungrounded wye connection through a grounding capacitor at the neutral point (Con2) and ungrounded wye connection through a low ratio current transformer (CT; Con3) are calculated as follows:

$$\begin{bmatrix}K_A\\K_B\end{bmatrix}=\begin{bmatrix}V_A^{\mathrm{re}}-V_{\mathrm{N}}^{\mathrm{re}} & V_B^{\mathrm{re}}-V_{\mathrm{N}}^{\mathrm{re}}\\ V_A^{\mathrm{im}}-V_{\mathrm{N}}^{\mathrm{im}} & V_B^{\mathrm{im}}-V_{\mathrm{N}}^{\mathrm{im}}\end{bmatrix}^{-1}\begin{bmatrix}V_{\mathrm{N}}^{\mathrm{re}}(1+K_{\mathrm{N}})-V_C^{\mathrm{re}}\\ V_{\mathrm{N}}^{\mathrm{im}}(1+K_{\mathrm{N}})-V_C^{\mathrm{im}}\end{bmatrix} \tag{5}$$

$$\begin{bmatrix}K_A\\K_B\end{bmatrix}=\begin{bmatrix}V_A^{\mathrm{re}}-V_{\mathrm{N}}^{\mathrm{re}} & V_B^{\mathrm{re}}-V_{\mathrm{N}}^{\mathrm{re}}\\ V_A^{\mathrm{im}}-V_{\mathrm{N}}^{\mathrm{im}} & V_B^{\mathrm{im}}-V_{\mathrm{N}}^{\mathrm{im}}\end{bmatrix}^{-1}\begin{bmatrix}V_{\mathrm{N}}^{\mathrm{re}}(1+K_{\mathrm{CT}})-V_C^{\mathrm{re}}\\ V_{\mathrm{N}}^{\mathrm{im}}(1+K_{\mathrm{CT}})-V_C^{\mathrm{im}}\end{bmatrix} \tag{6}$$

where K_{N} and K_{CT} are expressed as follows:

$$K_{\mathrm{N}}=\frac{C_{\mathrm{N}}}{C_C} \tag{7a}$$

$$K_{\mathrm{CT}}=\frac{-\mathrm{j}}{C_C\times 2\pi f\times CTR^2\times R_{\mathrm{b}}} \tag{7b}$$

It should be noted that C_{N} is assumed to be about 10% of C_C [24]. It should be mentioned that besides the cost issue, the greater neutral capacitor will increase the stored energy, and consequently enhances the chance of damage to the connected measuring devices. Note that the lower neutral capacitor will increase the noise level. It is also worth noting that the different values of C_N do

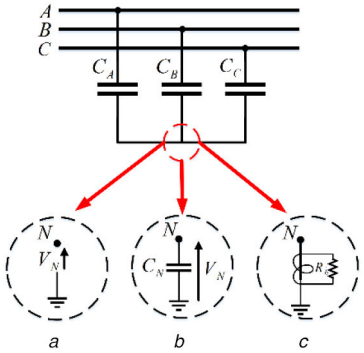

Fig. 1 *Different SCB configurations*
(a) Ungrounded wye connection, ***(b)*** Ungrounded wye connection through a grounding capacitor at the neutral point, ***(c)*** Ungrounded wye connection through a low ratio current transformer

Table 1 K-factor conditions for identifying faulty phases regarding internal fuse protection of SCBs

Item	K-factors condition	Faulty phases	New capacitance value for faulty phases
1	$K_A^{new} > K_A^{old}$ & $K_B^{new} \le K_B^{old}$	*B*, *C*	$\frac{C_c^{new}}{C_c^{old}} = \frac{K_B^{old}}{K_B^{new}}$ $\frac{C_a^{new}}{C_a^{old}} = \frac{K_B^{old}}{K_B^{new}} \times \frac{K_A^{new}}{K_A^{old}}$
2	$K_B^{new} > K_B^{old}$ & $K_A^{new} \le K_A^{old}$	*A*,*C*	$\frac{C_c^{new}}{C_c^{old}} = \frac{K_A^{old}}{K_A^{new}}$ $\frac{C_b^{new}}{C_b^{old}} = \frac{K_A^{old}}{K_A^{new}} \times \frac{K_B^{new}}{K_B^{old}}$
3	$K_B^{new} > K_B^{old}$ $K_A^{new} > K_A^{old}$ if $\left\{\left\lvert\frac{K_A^{old}}{K_A^{new}} - \frac{K_B^{old}}{K_B^{new}}\right\rvert < TR_1\right\}$	*C*	$\frac{C_c^{new}}{C_c^{old}} = \frac{K_A^{old}}{K_A^{new}}$
4	if $\left\{\frac{K_A^{old}}{K_A^{new}} < \frac{1}{TR_2} \times \frac{K_B^{old}}{K_B^{new}}\right\}$	*B*,*C*	same as item 1
5	if $\left\{\frac{K_B^{old}}{K_B^{new}} < \frac{1}{TR_2} \times \frac{K_A^{old}}{K_A^{new}}\right\}$	*A*,*C*	same as item2
6	$K_A^{new} < K_A^{old}$ & $K_B^{new} = K_B^{old}$	*A*	$\frac{C_a^{new}}{C_a^{old}} = \frac{K_A^{new}}{K_A^{old}}$
7	$K_B^{new} < K_B^{old}$ & $K_A^{new} = K_A^{old}$	*B*	$\frac{C_b^{new}}{C_b^{old}} = \frac{K_B^{new}}{K_B^{old}}$
8	$K_B^{new} < K_B^{old}$ & $K_A^{new} < K_A^{old}$	*A*, *B*	

Table 2 K-factor conditions for identifying faulty phases in externally fused and fuseless SCBs protection

Item	K-factors condition	Faulty phases	New capacitance value for faulty phases
1	$K_A^{new} < K_A^{old}$ & $K_B^{new} \ge K_B^{old}$	*B*, *C*	$\frac{C_c^{new}}{C_c^{old}} = \frac{K_B^{old}}{K_B^{new}}$ $\frac{C_a^{new}}{C_a^{old}} = \frac{K_B^{old}}{K_B^{new}} \times \frac{K_A^{new}}{K_A^{old}}$
2	$K_B^{new} < K_B^{old}$ & $K_A^{new} \ge K_A^{old}$	*A*, *C*	$\frac{C_c^{new}}{C_c^{old}} = \frac{K_A^{old}}{K_A^{new}}$ $\frac{C_b^{new}}{C_b^{old}} = \frac{K_A^{old}}{K_A^{new}} \times \frac{K_B^{new}}{K_B^{old}}$
3	$K_B^{new} < K_B^{old}$ $K_A^{new} < K_A^{old}$ if $\left\{\left\lvert\frac{K_B^{old}}{K_A^{new}} - \frac{K_B^{old}}{K_B^{new}}\right\rvert < TR_1\right\}$	*C*	$\frac{C_c^{new}}{C_c^{old}} = \frac{K_A^{old}}{K_A^{new}}$
4	if $\left\{\frac{K_A^{old}}{K_A^{new}} > \frac{1}{TR_2} \times \frac{K_B^{old}}{K_B^{new}}\right\}$	*B*, *C*	same as item 1
5	if $\left\{\frac{K_B^{old}}{K_B^{new}} > \frac{1}{TR_2} \times \frac{K_A^{old}}{K_A^{new}}\right\}$	*A*, *C*	same as item 2
6	$K_A^{new} > K_A^{old}$ & $K_B^{new} = K_B^{old}$	*A*	$\frac{C_a^{new}}{C_a^{old}} = \frac{K_A^{new}}{K_A^{old}}$
7	$K_B^{new} > K_B^{old}$ & $K_A^{new} = K_A^{old}$	*B*	$\frac{C_b^{new}}{C_b^{old}} = \frac{K_B^{new}}{K_B^{old}}$
8	$K_B^{new} > K_B^{old}$ & $K_A^{new} > K_A^{old}$	*A*, *B*	

not impact the formulation or the procedure of the capacitor unit failure detection method. The variations of C_C, even due to capacitor unit failure are negligible, as a result, K_N is assumed to have a constant value.

2.2 Faulty phase identification criteria

In the previous sub-section, the *k*-factors regarding different configurations of SCBs were introduced. However, it should be mentioned that regardless of SCB configurations, they may benefit from a fuse protection scheme, resulting in various conditions associated with the identification of faulty phases. To provide some criteria for identifying faulty phases of SCBs, some assumptions are used, which are described as follows:

- Firstly, it is assumed that the capacitor failures will not occur simultaneously in all three phases. It should be mentioned that the scheme presented in [23] has also made this assumption in the calculations. However, it is worth mentioning that unlike [7], the proposed method can identify multiple capacitor unit failures in the case of two faulty phases.
- The second assumption in this algorithm is regarding the internal fuse configuration of SCB. It is assumed that the capacitor is decreased after the operation of the fuse. While in fuseless SCBs, after fault occurrence, the capacitor is increased. In SCBs with external fuse configuration, the capacitor of the SCB is increased in each phase at first, but after external fuse operation, the equivalent capacitor is decreased.

Based on the above-mentioned assumptions, the fault detection algorithms for different fuse protections of SCBs are given in Tables 1 and 2.

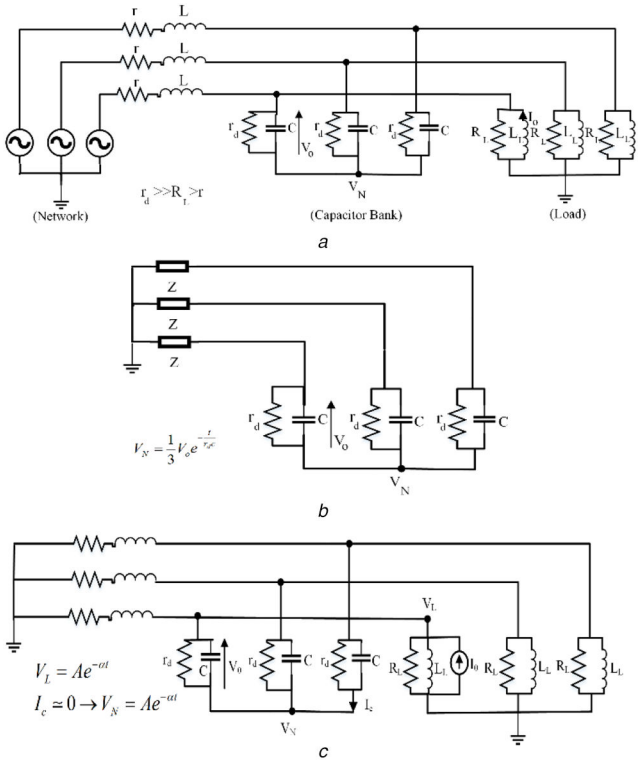

Fig. 2 *Illustration of a simple three-phase power system with an SCB*
(a) General illustration of the system, ***(b)*** Equivalent circuit for the effect of the capacitor residual voltage on the neutral voltage, ***(c)*** Equivalent circuit for the effect of the inductance residual current on the neutral voltage

2.3 Determining the number of failed elements in each phase of the SCB

The number of failed elements is determined based on the variations of the total capacitance elements, before and after the internal fault, and the failed elements in each phase of the SCB. N_e denotes the total number of elements for the SCBs in each phase, during healthy condition. Considering Q_e as the reactive power of each element, the reactive power of the SCB in each phase before element failure (Q_{old}) and after element failure (Q_{new}) are calculated as follows:

$$Q_{old} = C_{old}V_{old}^2 \simeq N_e^{old} \times Q_e \tag{8a}$$

$$Q_{new} = C_{new}V_{new}^2 \simeq \theta N_e^{new} \times Q_e \tag{8b}$$

In (8a) and (8b), it is assumed that the average value of reactive power after element failure occurrence remains close to its nominal value. As a result, the number of failed elements (N_d) is calculated as follows:

$$\frac{C_{new}}{C_{old}} = \frac{N_e^{new}}{N_e^{old}} \times \left(\frac{V_{old}}{V_{new}}\right)^2$$
$$\Rightarrow N_d = N_e^{old} - N_e^{new} = \left(1 - \frac{N_e^{new}}{N_e^{old}} \times \left(\frac{V_{old}}{V_{new}}\right)^2\right) N_e^{old} \tag{9a}$$

$$N_e^{new} = N_e^{old} - N_d \tag{9b}$$

$$N_e = N_s \times N_p \times N_{us} \times N_{up} \times N_{br} \tag{9c}$$

where N_d is the number of failed elements, N_s is the number of series sections in each unit, N_p is the number of parallel elements in each series section of each unit, N_{us} is the number of series sections of each capacitor unit per branch in each phase, N_{up} is the number of parallel units in each series section of units, and N_{br} is the number of unit branches in each phase. The superscripts 'old' and 'new' denote the status before and after the internal fault.

2.4 Temporary external short circuit fault effect on SCBs

Most of the suggested and concluded expressions in the previous subsections and also previous related published methods [7] are based on the fundamental phasor component of the voltage signal. DFT is one of the most famous phasor estimation algorithms widely utilised in digital relays for the calculation of the fundamental phasor component. However, as discussed in [25], there are several issues that could result in the inaccuracy of DFT due to the nature of the signal. The inaccuracy in calculation of the DFT will be reflected in the fundamental phasor component and may result in the addition of an unwanted delay or even maloperation of the digital relays. As a result, it is obvious that the phasor estimator should be equipped with proper auxiliary filters for dealing with disturbing transient components being generated from abnormal operating conditions.

Temporary external unbalanced short circuit faults may result in the generation of decaying transients in the neutral voltage of the SCBs. These transients definitely and profoundly affect the performance of the conventional DFT calculations. More importantly, such a situation may result in the occurrence of overvoltages in other unfaulty phases, which may lead to single or multiple capacitor unit failure(s). As a result, it is vital to deal with the inaccuracy in the estimated fundamental component of the voltage. In the following, first, based on the superposition theorem in circuit analysis, the nature of the transients is mathematically modelled. After that, an auxiliary filter is introduced to enhance the immunity of the conventional DFT calculations to the aforementioned transients. Fig. 2*a* shows the schematic of a simple three-phase power system containing an SCB. According to Fig. 2*a*, during a temporary fault condition, the capacitor unit and the inductance of the load may contain residual voltage and current components, respectively. Obviously, these residual components get damped after some cycles. The neutral voltage waveform is generally expressed as follows:

$$v_n(t) = v_{n,s}(t) + v_{n,cap}(t) + v_{n,ind}(t) \tag{10}$$

where $v_n(t)$, $v_{n,s}(t)$, $v_{n,cap}(t)$, and $v_{n,ind}(t)$ denote the total neutral voltage, neutral voltage due to the voltage source, neutral voltage due to the capacitor residual voltage, and neutral voltage due to the inductance residual current, respectively.

To obtain a mathematical description for the effects of the source voltage, the inductance residual current, and the capacitor residual voltage on the neutral voltage, utilising the superposition theorem in circuit analysis, the following can be concluded.

2.4.1 Effect of voltage source on the neutral voltage: It is obvious that the general form of the neutral point voltage is similar to the voltage source. In other words, any harmonic component regarding the voltage source is reflected in the neutral point voltage waveform. As a result, the voltage waveform of the neutral point considering the voltage source effect is generally expressed as follows:

$$v_{n,s}(t) = \sum_{i=1}^{h} V_{n,i}\sin(2\pi fit + \theta_{n,i}) \tag{11}$$

where $V_{n,i}$, and $\theta_{n,i}$ are the magnitude and the phase angle of the ith harmonic component of the neutral voltage waveform. Also, f is the system frequency and it is equal to 50 Hz.

2.4.2 Effect of capacitor residual voltage on the neutral voltage: The equivalent circuit used to describe this condition is shown in Fig. 2*b*. According to Fig. 2*b*, the expression for $v_{n,cap}(t)$ can be obtained as

$$v_{\mathrm{n,cap}}(t) = V_{\mathrm{n,cap},0}\mathrm{e}^{-t/\tau_{\mathrm{c}}}$$
$$\tau_{\mathrm{c}} = \left(r_{\mathrm{d}} + \left(\frac{R_{\mathrm{L}} \times r}{R_{\mathrm{L}} + r}\right)\right)C \tag{12}$$

where $V_{\mathrm{n,cap},0}$, τ_{c}, and C are the voltage magnitude at the neutral point due to the capacitor residual voltage, the circuit time constant, and the equivalent capacitor of the SCB for one phase. Also, r_{d}, R_{L}, and r are the resistances regarding the SCB, load, and source, respectively. According to [25], the value of R_{s} is much greater than r and R_{L}, and thus, τ_{c} is in order of minutes. Since the window length for the calculation of DFT is equal to one cycle (20 ms), $v_{\mathrm{n,cap}}(t)$ can be approximately assumed a constant value during one cycle. Hence, the expression (12), can be rewritten as follows:

$$v_{\mathrm{n,cap}}(t) = V_{\mathrm{n,cap},0} \tag{13}$$

2.4.3 Effect of inductance residual current on the neutral voltage: Similar to the previous discussion regarding the residual voltage of the capacitor, the equivalent circuit of the inductance residual current is shown in Fig. 2*c*. According to Fig. 2*c*, the expression for $v_{\mathrm{n,ind}}(t)$ can be obtained as

$$v_{\mathrm{n,ind}}(t) = V_{\mathrm{n,ind},0}\mathrm{e}^{-t/\tau_{\mathrm{L}}}$$
$$\tau_{\mathrm{L}} = \frac{(R_{\mathrm{s}} + R_{\mathrm{L}})L}{R_{\mathrm{s}} \times R_{\mathrm{L}}} \tag{14}$$

where $V_{\mathrm{n,ind},0}$, τ_{L}, and L are the voltage magnitude at the neutral point due to the load inductance residual current, the circuit time constant, and the load inductance for one phase.

Based on the above discussion and (10)–(14), the general form of the neutral voltage waveform is expressed as follows:

$$v_{\mathrm{n}}(t) = V_{\mathrm{n},0} + V'_{\mathrm{n},0}\mathrm{e}^{-\alpha t} + \sum_{i=1}^{h} V_{\mathrm{n},i}\sin(2\pi \mathrm{f} i t + \theta_{\mathrm{n},i}) \tag{15}$$

To remove the effect of DC terms, applying integration in (15) over one cycle, it can be written as follows:

$$\begin{aligned} X_1 &= \int_0^T v_{\mathrm{n}}(t)\mathrm{d}t \\ &= \int_0^T (V_{\mathrm{n},0} + V'_{\mathrm{n},0}\mathrm{e}^{-\alpha t} + \sum_{i=1}^{h} V_{\mathrm{n},i}\sin(2\pi \mathrm{f} i t + \theta_{\mathrm{n},i}))\mathrm{d}t \\ &= \int_0^T V_{\mathrm{n},0}\mathrm{d}t + \int_0^T V'_{\mathrm{n},0}\mathrm{e}^{-\alpha t}\mathrm{d}t + \int_0^T \sum_{i=1}^{h} V_{\mathrm{n},i}\sin(2\pi \mathrm{f} i t + \theta_{n,i})\mathrm{d}t \\ &= \int_0^T V_{\mathrm{n},0}\mathrm{d}t + \int_0^T V'_{\mathrm{n},0}\mathrm{e}^{-\alpha t}\mathrm{d}t \\ &= V_{\mathrm{n},0}T - \frac{V'_{\mathrm{n},0}}{\alpha}(\mathrm{e}^{-\alpha T} - 1) \end{aligned} \tag{16}$$

By shifting the integration window by Δt and $2\Delta t$, and repeating (16), the following expressions are obtained:

$$X_2 = \int_{\Delta t}^{T+\Delta t} v_{\mathrm{n}}(t)\mathrm{d}t = V_{\mathrm{n},0}T - \frac{V'_{\mathrm{n},0}}{\alpha}(\mathrm{e}^{-\alpha T} - 1)\mathrm{e}^{-\alpha \Delta t} \tag{17}$$

$$X_3 = \int_{2\Delta t}^{T+2\Delta t} v_{\mathrm{n}}(t)\mathrm{d}t = V_{\mathrm{n},0}T - \frac{V'_{\mathrm{n},0}}{\alpha}(\mathrm{e}^{-\alpha T} - 1)\mathrm{e}^{-2\alpha \Delta t} \tag{18}$$

From (16)–(18), α, $V'_{\mathrm{n},0}$, and $V_{\mathrm{n},0}$ are calculated as follows:

$$\alpha = \frac{-1}{\Delta t}\ln\left(\frac{X_3 - X_2}{X_2 - X_1}\right) \tag{19}$$

$$V'_{\mathrm{n},0} = \frac{\alpha(X_2 - X_1)}{(\mathrm{e}^{-\alpha T} - 1)(1 - \mathrm{e}^{-\alpha \Delta t})} \tag{20}$$

$$V_{\mathrm{n},0} = \frac{1}{T}\left(X_1 + \frac{V'_{\mathrm{n},0}}{\alpha}(\mathrm{e}^{-\alpha T} - 1)\right) \tag{21}$$

After calculating α, $V'_{\mathrm{n},0}$, and $V_{\mathrm{n},0}$, the DC terms can be removed from $v_{\mathrm{n}}(t)$ as follows:

$$\begin{aligned} v_{\mathrm{n}}^{\mathrm{new}}(t) &= v_{\mathrm{n}}(t) - (V_{\mathrm{n},0} + V'_{\mathrm{n},0}\mathrm{e}^{-\alpha t}) \\ &= \sum_{i=1}^{h} V_{\mathrm{n},i}\sin(2\pi \mathrm{f} i t + \theta_{\mathrm{n},i}) \end{aligned} \tag{22}$$

In this stage, by applying DFT in (22), the fundamental phasor voltage component of the neutral point can be estimated without the unwanted effects of the DC terms.

3 Implementation

This section describes the implementation procedure of the proposed algorithm for capacitor element failure detection in the SCBs. In this study, the test systems are implemented in PSCAD to obtain the signals required for the proposed algorithm, whilst the proposed algorithm is implemented in MATLAB.

The proposed method basically conducts its calculation based on the phasor component. The fundamental phasor component is calculated based on the discrete Fourier algorithm. Comparing the frequency range of the travelling wave, and the window length required for phasor calculation, the impact of very high-frequency is automatically ignored in the calculation. Even if the high-frequency components are very impactful, the phasor calculation procedure is performed for consecutive windows of data (i.e. window length assumed 1 ms) so that the error of calculated phasor in two consecutive windows becomes <0.01%.

Depending on the SCB configuration, the neutral voltage and/or current signals are required as the input data of the proposed algorithm.

For each fault scenario, i.e. analysed by the proposed algorithm, the following steps should be applied:

Step 1 (initialisation): in this step, the requirements of the SCB model including the type of SCB, the number of elements and units, and other information regarding the power network for the simulation are entered in PSCAD-based network.

Step 2 (simulation in PSCAD): using the PSCAD simulation environment, the simulation is performed with a 1 μs step time. For each time step of the simulation, the phase and neutral voltage/current signals are transferred to the MATLAB environment to perform the proposed algorithm.

Step 3 (phasor calculation): since the proposed method conducts its calculation based on the fundamental component, it is essential to calculate the fundamental phasor component from the signal. Therefore, by using (15)–(22), the fundamental voltage (or current) component is calculated. Note that the sampling rate required to apply the phasor calculation is adjusted to 100 μs.

Step 4 (K-factor calculation): based on the phasor calculated in step 3, the K-factors are calculated using (4), (5), or (6).

Step 5 (prevent negative impact of transients): owing to the unwanted impact that may be imposed by transients during external faults, the calculated $K(t)$ is compared with the previous stage until the variation of $K(t)$ from two consequent steps of $K(t)$ (i.e. 100 μs) becomes lower than α. Note that α is assumed 0.0001.

Step 6 (fault location): once $K(t)$ applies in the criterion of step 5, the fault location is determined using the obtained $K(t)$. Note that the fault location is determined based on the expressions in Tables 1 and 2.

Step 7 [number of failed element (NoFE) calculation]: based on the new value of the capacitor, NoFE is calculated using (9).

Step 8 (updating K-factors): finally, K-factors are updated for the next simulation step time and the algorithm is repeated until the end of the simulation.

It should be noted that steps 1 and 2 are performed in PSCAD whilst the proposed algorithm is implemented in MATLAB environment (see Fig. 3).

4 Performance evaluation of the proposed method

To evaluate the performance of the proposed method, several case studies under different circumstances and for different system grounding of SCBs are discussed. Several scenarios including consecutive element failures, simultaneous element failures in one phase, and simultaneous element failures on multiple phases are observed. The test system shown in Fig. 4 is utilised for the simulation of the cases, except for the case of the CB with an external fuse. All simulations are performed in PSCAD and MATLAB simulation environment. The specifications of the test system are given in Table 3.

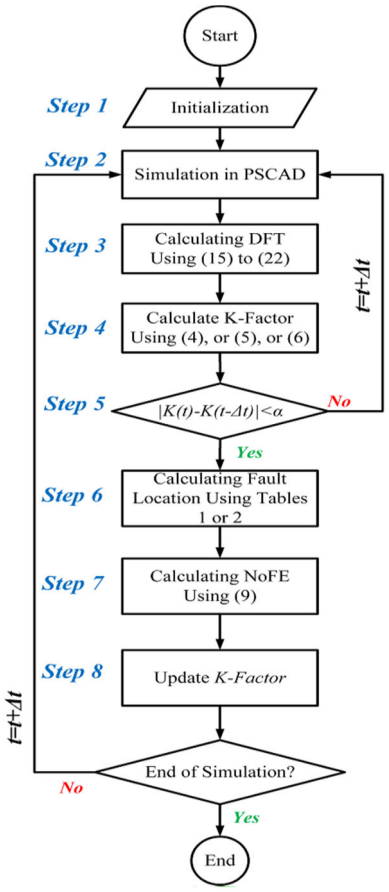

Fig. 3 *Implementation flowchart of the proposed algorithm*

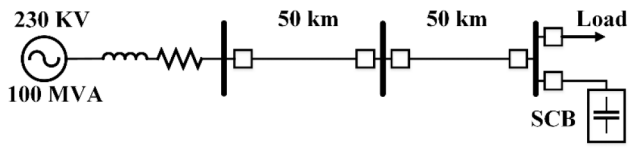

Fig. 4 *Single line diagram of the test system*

As can be seen in Fig. 4, the test system is provided with an SCB to study both the internally fused and the fuse-less configurations of the SCBs. The specifications of the desired SCB configurations are given in Table 4. It should be mentioned that the grounding systems in the configurations illustrated in Fig. 5 consists of isolated, solidly grounded, grounded with a capacitor, and grounded with CT.

To show the capability of the proposed method, the monitoring of the desired parameters including the detection of the faulty phase, the estimation of the number of failed elements in the faulty phases and the determination of the failed capacitors in each phase is analysed for each time step of the simulation for all case studies.

4.1 Star connection SCBs with ungrounded neutrals

Table 5 shows the specifications for the fault scenarios regarding an internally fused ungrounded SCB. It should be noted that the fault scenarios are not necessarily in a specific unit and may be in different units, leading to excessive difficulty in SCB monitoring. To address the failed elements in an SCB, three parameters including fault inception time (FIT), fault detection time (FDT), and NoFE are specified in the figures depicting the simulation results. These parameters are described as follows:

FIT: The instant at which the fault is applied and a certain number of elements are shorted.
FDT: The instant at which the proposed method successfully detects the failed elements.
NoFE: This parameter is calculated based on (9) to show whether the calculated NoFE is equal to applied failures.

Fig. 6*a* shows neutral voltage signals regarding the scenarios given in Table 5. As can be seen in Fig. 6*a*, due to each unit failure specified in Table 5, the neutral voltage signal experiences different levels of variations. Fig. 6*a* shows the capacitor element failures in an SCB. However, it is unclear how many elements failed in each phase.

According to Fig. 6*b*, the proposed algorithm detects the elements failed in each phase with almost one cycle delay. For instance, according to Table 5, the failure in the first scenario has occurred at $t = 0.15$ s with the NoFE for phases A, B, and C being 1, 0, and 2, respectively. As can be seen in Fig. 6*b*, the proposed algorithm detects the failed elements at $t = 0.17$ s (with one cycle delay) and the NoFE calculated by the proposed method matches the quantities in Table 5. As illustrated in Fig. 6*b*, the proposed method can track the element failures exactly as considered for each scenario in Table 5. From Fig. 6*b*, it is obvious that the proposed method can detect the element failures, which simultaneously occurred in two phases.

Also, as can be seen in Fig. 6*a* that between 0.25 and 0.3 s, the fundamental component of the neutral voltage signal has a zero value, however, according to Table 5, some elements are failed. As can be seen in Fig. 6*b*, the proposed method detects the element failures in phases A, B, and C; being in consistency with Table 5.

Table 3 Specifications of the test system given in Fig. 4

source impedance	$Z_1 = 1.5 + j10,\ Z_0 = 15 + j30$
external impedance	$5 + j5$
balanced load	120 MW, 0.9 Lag
transmission lines	$Z_1 = 25.45\angle 85.9°, Z_0 = 68.76\angle 74.6°$
CB	70 MVAR

Table 4 Specifications of the internally fused and fuse-less SCBs

Bank type	S	P	U_S	U_P	br	$C_{element}$, μf
internal fuse	3	14	6	2	2	1.36
fuse less	6	1	12	1	5	60.8

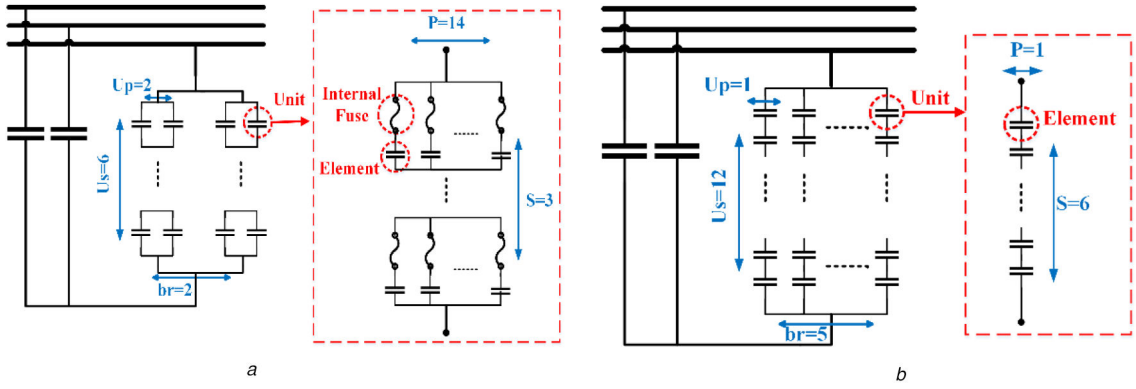

Fig. 5 *Detailed configuration of internally fused and fuseless SCBs*
(a) Illustration of internally fused SCB, ***(b)*** Illustration of fuseless SCB

Table 5 specifications of the fault scenarios for an internally fused ungrounded SCB

FIT, s	0.15	0.2	0.25	0.3	0.35	0.4	0.45
phase A	1	1	0	1	0	2	0
phase B	0	0	2	1	0	0	2
phase C	2	0	0	0	2	1	1

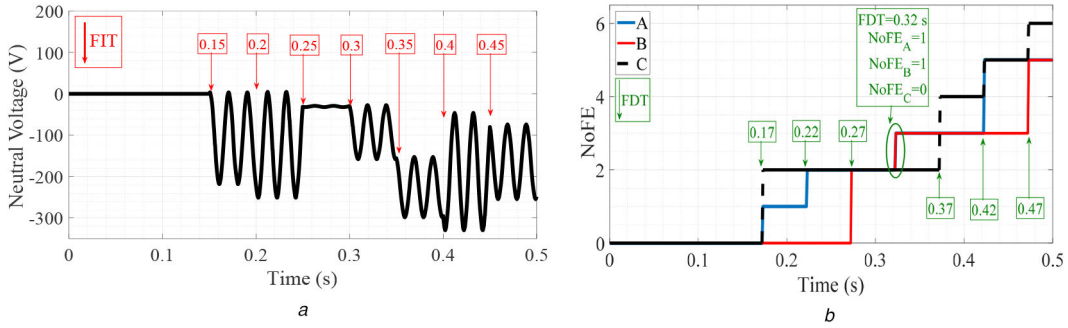

Fig. 6 *Performance of the proposed method in the case of an SCB with star connection and ungrounded neutral*
(a) Neutral voltage, ***(b)*** Failed elements

Table 6 Specifications of the fault in SCB

FIT, s	0.15	0.2	0.3	0.35	0.4	0.45
phase A	0	2	1	0	1	1
phase B	2	0	1	1	0	2
phase C	2	1	0	2	1	0

It is noteworthy that the zero value in Fig. 6*a* will lead to maloperation of the SCB relay in element failure detection, and consequently, the maloperation of the capacitor bank (CB) [23]. However, the proposed algorithm can deal with the aforementioned issues with very good accuracy.

4.2 Star connection of the SCB with neutral capacitor grounding

The specifications of the element failure scenarios for an internally fused SCB with neutral capacitor grounding are provided in Table 6.

The same as the previous case study, different scenarios that are applied to the SCB are given in Table 6. The scenarios are designed to show the performance of the proposed algorithm in the case of simultaneous element failures in multiple phases.

Fig. 7*a* shows the neutral voltage signal before and after applying the element failures to the SCB. As can be seen in Fig. 7*b*, the proposed method detects and tracks element failures very accurately and in agreement with Table 6. For instance, as illustrated in Fig. 7*b*, the NoFEs for phases *A*, *B*, and *C* regarding the scenario being applied at $t = 0.2$ match to the data in Table 6. Overall, just as the previous case study, it can be concluded that the proposed method can detect and monitor the condition of the capacitor grounded SCB during capacitor failures in the case of involving multiple phases simultaneously.

4.3 SCBs with star connection and neutral CT grounding

The specification of the fault scenarios for an internally fused SCB with neutral CT grounding is provided in Table 7. The selected CT in this study has a ratio of 50/5 and a 10-Ω burden [7].

Fig. 8*a* illustrates the natural current regarding an SCB with CT grounding considering different element failure scenarios. As can be seen in Fig. 8*b*, the proposed method precisely detects and tracks the failed elements in each scenario with only one cycle delay with respect to the FITs shown in Table 7. As mentioned before, the proposed method operates based on the fundamental voltage component. It is obvious that the calculation of the fundamental voltage component with DFT is associated with one cycle delay. Note that in the case of neutral grounding with a CT, the neutral current signal is converted to a voltage signal and then is applied to the proposed method. Regarding this case study, the proposed method is able to deal with simultaneous element failures in multiple phases.

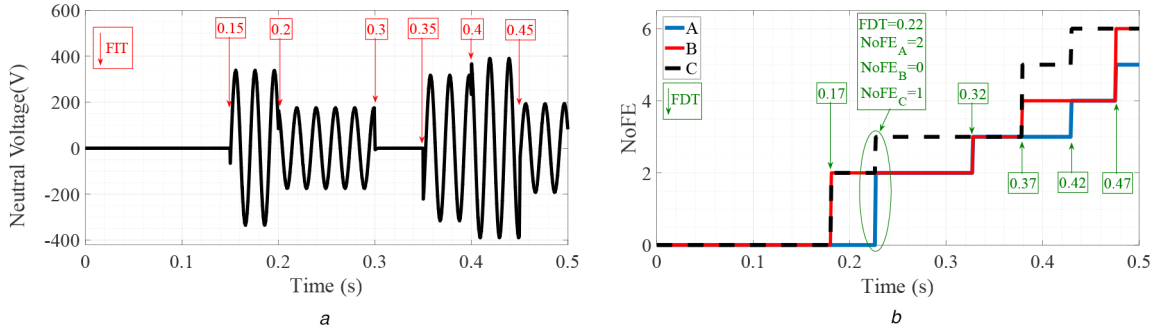

a *b*

Fig. 7 *Performance of the proposed method in the case of a star connection SCB with neutral capacitor grounding*
(a) Neutral voltage, ***(b)*** Failed elements

Table 7 Specifications of the fault in CB

FIT, s	0.15	0.2	0.25	0.3	0.4
phase A	0	2	1	0	1
phase B	3	0	0	1	0
phase C	1	1	1	2	2

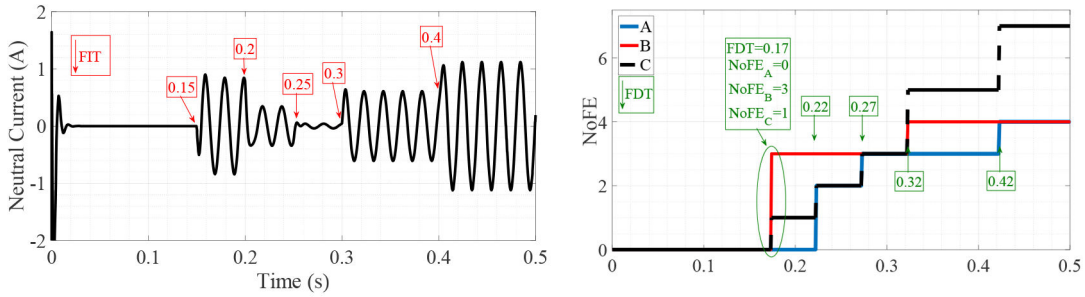

a *b*

Fig. 8 *Performance of the proposed method in the case of SCBs with star connection and neutral CT grounding*
(a) Neutral current, ***(b)*** Failed elements

Table 8 Levels of imbalance and the injected harmonics in the applied voltage

Phases	Fundamental component, kV	Fifth harmonic (% of fundamental component)	Seventh harmonic (% of fundamental component)	11th harmonic (% of fundamental component)
a	$230/\sqrt{3}\angle 10$	$0.35U_N\angle 10$	$0.2U_N\angle 80$	$0.07U_N\angle 45$
b	$253/\sqrt{3}\angle -150$	$0.18U_N\angle -32$	$0.12U_N\angle -59$	$0.09U_N\angle -142$
c	$207/\sqrt{3}\angle 100$	$0.24U_N\angle 165$	$0.04U_N\angle 56$	$0.06U_N\angle 48$

4.4 Effects of harmonics and unbalanced voltages

Similar to Sections 4.1–4.3, the performance of the proposed method is investigated regarding a fuseless SCB with a capacitor grounded under non-sinusoidal conditions. The specifications for the scenarios are given in Table 6. Moreover, the levels of imbalance and the injected harmonics in the applied voltage are tabulated in Table 8.

As is clear in Fig. 9*d*, the proposed method tracks the correct number of element failures with one cycle delay. As a result, it can be concluded that the proposed method shows robust performance under harmonic polluted and imbalance voltage signals.

4.5 Effect of the power grid short circuit faults

In this section, the performance of the proposed method during short circuit faults in a power grid is investigated. In this situation, it can be expected that the neutral voltage or current experience a significant enhancement due to the decaying DC component. As a result, the monitoring algorithms falsely assume that several elements are failing.

To deal with this situation, a criterion is provided by the proposed algorithm, which suspends the procedure of updating the K-factors in case the neutral voltage suddenly rises up to 30% of the nominal voltage in each phase. This criterion, somehow acting as a short circuit detection method in the power grid, continues to suspend the K-factor calculations until the short circuit fault is cleared. After the fault clearance, K-factors will be updated using the pre-fault data to detect the potential element failure that may or may not have occurred during the short circuit fault in the power grid. For the sake of simulations, a single-phase ground fault is started at $t = 0.23$ s and removed at $t = 0.28$ s. The specifications for studying element failure in an ungrounded internally fused SCB in the case of an external short circuit fault are provided in Table 9. As can be seen in Fig. 10, the neutral voltage experiences a significant rise. After the fault clearance, the voltages of the different phases of the SCB are ought to be balanced. As a result, a transient unbalance overvoltage appears in the neutral of the SCB. After this transient overvoltage, the neutral voltage containing decaying DC components causes inaccuracy in the estimation of the fundamental component using conventional DFT, as shown in Fig. 6*b*. Nevertheless, as can be seen in Fig. 6*c*, using (15)–(22), the fundamental component of the neutral voltage signal can be appropriately calculated with maximum immunity to the decaying DC component.

4.6 Externally fused CBs

Consecutive element failures, which usually occur in SCBs with external fuses, will continuously occur until the fuse of the faulty unit melts [26]. In that case, an indication flag is raised, denoting

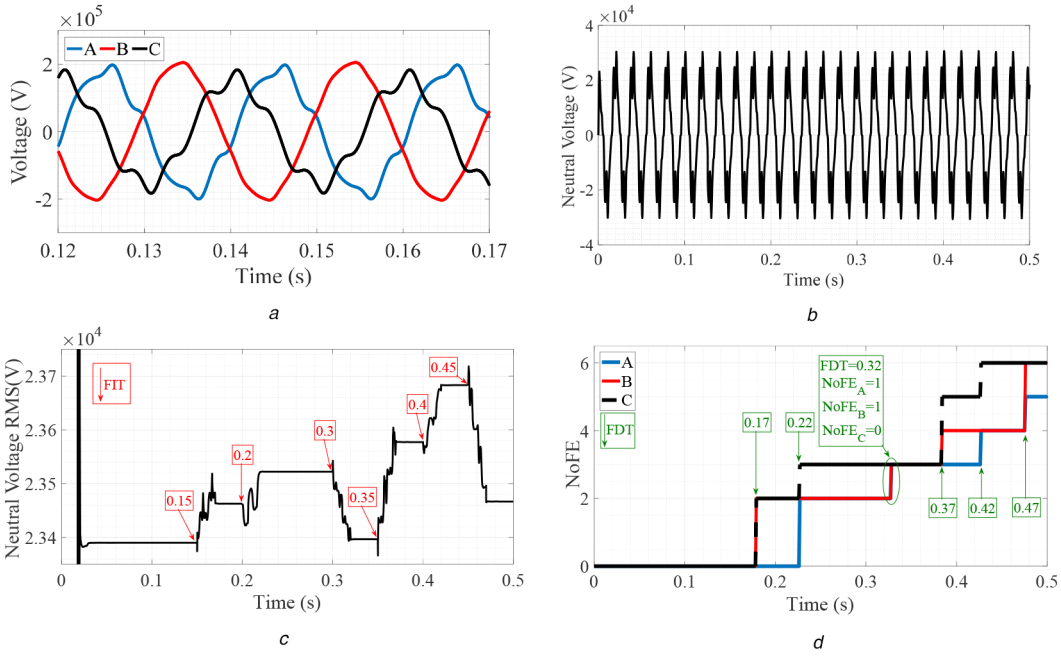

Fig. 9 *Performance of the proposed algorithm considering the effects of harmonics and unbalanced voltages*
(a) SCB phase voltages, ***(b)*** Neutral voltage, ***(c)*** Root mean square (RMS) of the fundamental harmonic of the neutral voltage, ***(d)*** Failed elements

Table 9 Specification of fault in SCB

FIT, s	0.15	0.2	0.25	0.4	0.45
phase A	1	1	1	2	0
phase B	0	0	3	1	2
phase C	2	0	0	0	1

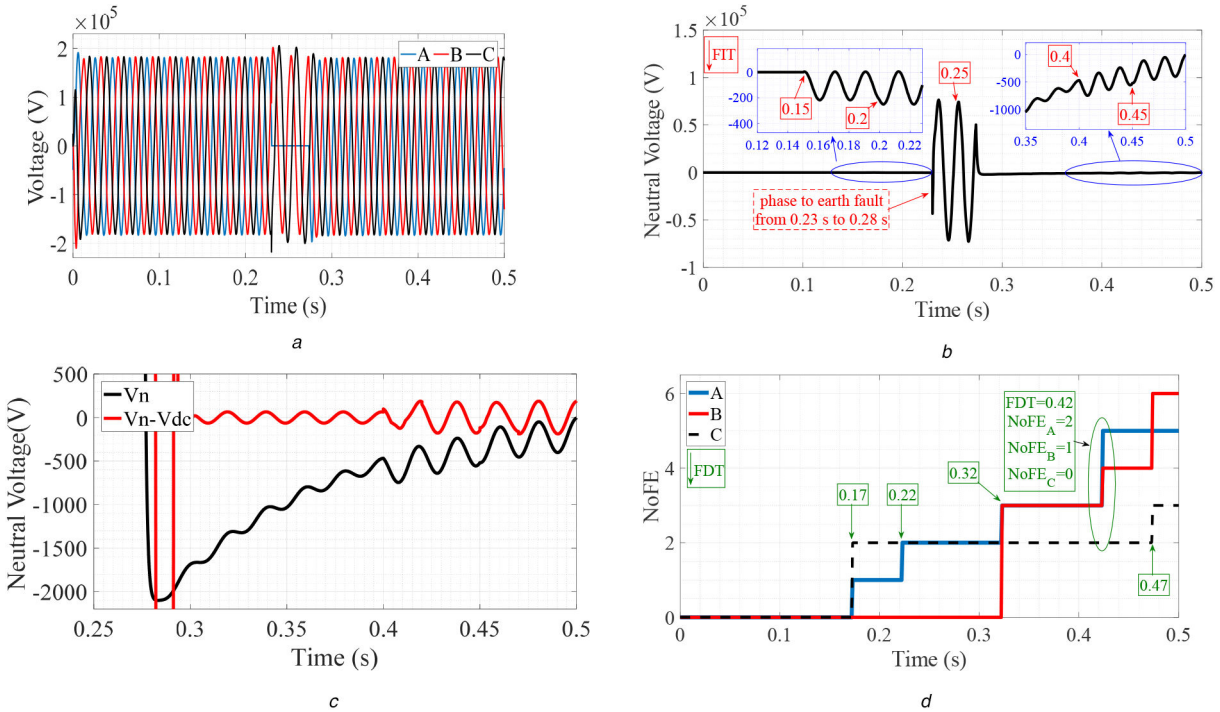

Fig. 10 *Performance of the proposed algorithm considering the effect of power grid short circuit faults*
(a) Phase voltages of the SCB, ***(b)*** Neutral voltage, ***(c)*** Fundamental harmonic of the neutral voltage with/without DC component ***(d)*** Failed elements

the faulty unit [14]. A series of test cases showing how the proposed method provides a fast and reliable solution to avoid melting of the external fuses are provided in this section. It is also worth noting that similar to the fuseless SCB, when an element fails in an SCB with external fuse, it means that the element is short-circuited. To verify the performance of the proposed method for SCBs with external fuses, a test case is provided, as depicted in Fig. 11. The specifications of the externally fused SCB and the scenarios considered through regarding case studies are given in Tables 10 and 11, respectively.

Fig. 12*a* shows that the voltage signal of the neutral is changed after applying the scenarios. The performance of the proposed algorithm is shown in Fig. 12*b*. As can be seen in Fig. 12*b*, the proposed method monitors the scenarios with high accuracy and

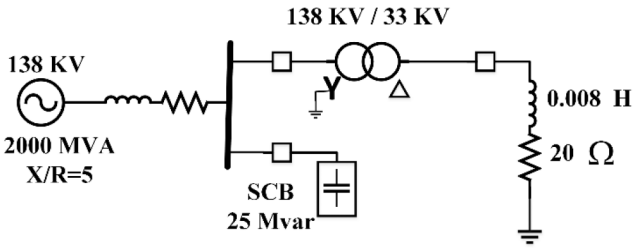

Fig. 11 *Test system for verification of the proposed method performance for an externally fused SCB*

Table 10 Specification for the SCB with external fuse

Bank type	*S*	*P*	U_s	U_P	br
external fuse	8	3	5	14	1

Table 11 Specification of fault scenarios for the externally fused SCB

FIT, s	0.15	0.2	0.3
phase A	0	4	1
phase B	4	0	2
phase C	2	4	0

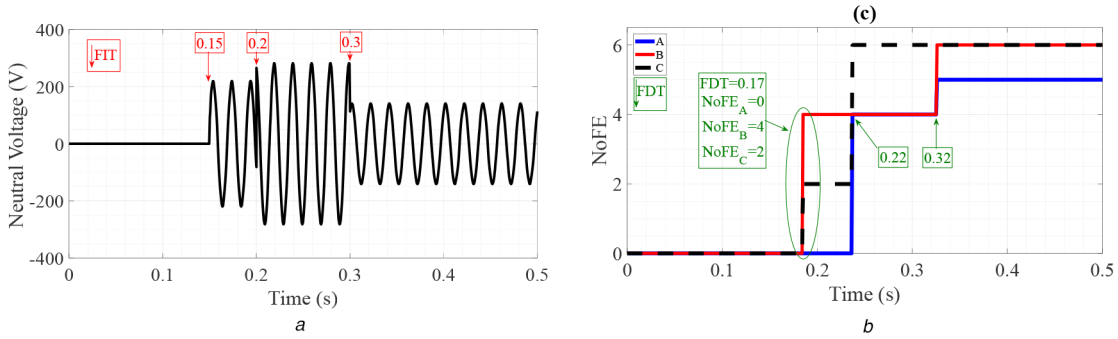

Fig. 12 *Performance of the proposed method for externally fused SCBs*
(a) Neutral voltage, ***(b)*** Number of failed elements in each phase

Table 12 Capabilities and salient features of the proposed method and the state-of-the-arts

		[16]	[12, 13]	[7]	Proposed method
number	C&SF	✓	✓	✓	✓
1	detecting faulty phases	✗	✗	✓	✓
2	detecting consecutive failures in a single phase	✗	✗	✓	✓
3	providing an advanced criterion for fuse-saving of externally fused SCBs	✗	✗	✓	✓
4	ability to deal with ambiguous failures	✗	✗	✓	✓
5	applicable for different SCB configurations	✗	✗	✓	✓
6	online monitoring of the number of failed elements	✗	✗	✓	✓
7	detecting the consecutive failures in two phases	✗	✗	✗	✓
8	dealing with the decaying DC component	✗	✗	✗	✓
9	robustness against voltage unbalance and harmonic polluted signals	✗	✗	✗	✓

total match to Table 11. Accordingly, the proposed method can overcome the challenges regarding this configuration of the SCBs.

4.7 Performance comparison of the SCB monitoring algorithms

To evaluate the performance of the proposed algorithm, several SCB element failure scenarios were applied to the proposed failure detection method. The capabilities and the salient features (C&SFs) of the proposed method and previously published methods in SCB element failure detection are summarised in Table 12. From Table 12, it can be observed that

- All methods are able to detect the faulty phases.
- The proposed method and also the methods in [7] possess the C&SFs 2–6 while the methods in [12, 13, 16] are unable to respond correctly to these conditions.

C&SFs 7–9 are the unit C&SFs that only the proposed method can deal with them. No discussions have been given in the previously published algorithms regarding these C&SFs.

To compare the performance of the proposed algorithm with the previously published papers, performance evaluations are conducted between the proposed method and the methods proposed in [7, 8], which are so far the most efficient algorithms. In this comparison, all six scenarios introduced in Sections 4.1–4.6 are applied to the suggested methods in [7,8]. The results are provided in Table 13. It should be noted that (*X*, *Y*, *Z*) shows the NoFE corresponding to each phase. The red font in Table 13 is representative of a failure in correct detection.

Table 13 Performance comparison between the proposed method and the methods presented in [7, 8]

Scenarios		Algorithm	FIT, s						
			0.15	0.2	0.25	0.3	0.35	0.4	0.45
4.1.	according to Table 5	[7, 8]	(0, 0, 1)	(1, 0, 0)	(0, 2, 0)	(0, 0, 1)	(0, 0, 2)	(1, 0, 0)	(1, 0, 0)
		proposed method	(1, 0, 2)	(1, 0, 0)	(0, 2, 0)	(1, 1, 0)	(0, 0, 2)	(2, 0, 1)	(0, 2, 1)
4.2.	according to Table 6	[7, 8]	(3, 0, 0)	(1, 0, 0)	(0, 0, 0)	(0, 0, 0)	(0, 0, 1)	(0, 1, 0)	(0, 1, 0)
		proposed method	(0, 2, 2)	(2, 0, 1)	(0, 0, 0)	(1, 1, 0)	(0, 1, 2)	(1, 0, 1)	(1, 2, 0)
4.3.	according to Table 7	[7, 8]	(0, 4, 0)	(1, 0, 0)	(0, 1, 0)	(0, 0, 2)	(0, 0, 0)	(0, 0, 1)	(0, 0, 0)
		proposed method	(0, 3, 1)	(2, 0, 1)	(1, 0, 1)	(0, 1, 2)	(0, 0, 0)	(1, 0, 2)	(0, 0, 0)
4.4.	according to Table 6	[7, 8]	(0, 0, 0)	(0, 0, 0)	(0, 0, 0)	(0, 0, 0)	(0, 0, 0)	(0, 0, 0)	(0, 0, 0)
		proposed method	(0, 2, 2)	(2, 0, 1)	(0, 0, 0)	(1, 1, 0)	(0, 1, 2)	(1, 0, 1)	(1, 2, 0)
4.5.	according to Table 9	[7, 8]	(0, 0, 2)	(1, 0, 0)	(0, 0, 0)	(0, 0, 0)	(0, 0, 0)	(0, 0, 0)	(0, 0, 0)
		proposed method	(1, 0, 2)	(1, 0, 0)	(1, 3, 0)	(0, 0, 0)	(0, 0, 0)	(2, 1, 0)	(0, 2, 1)
4.6.	according to Table 11	[7, 8]	(0, 5, 0)	(0, 7, 0)	(0, 0, 0)	(0, 1, 0)	(0, 0, 0)	(0, 0, 0)	(0, 0, 0)
		proposed method	(0, 4, 2)	(4, 0, 4)	(0, 0, 0)	(1, 2, 0)	(0, 0, 0)	(0, 0, 0)	(0, 0, 0)

As can be seen in Table 13, the following is concluded:

- For scenarios 4.1–4.3 and 4.6, the proposed method successfully detects all failures, in contrast to the methods [7, 8], which failed to correctly detect NoFE. The reason for failure in [7, 8] is that these methods can only deal with just one failure in one phase, whilst in the observed scenarios, multiple failures have occurred in several phases.
- In scenario 4.6, the suggested methods in [7,8] cannot deal with the level of voltage unbalance and also the harmonic levels are higher than the permissible level. While the proposed method can successfully deal with any level of voltage unbalance and harmonic contents, even higher than permissible level, which may occur in case of using a static var compensators or harmonic filters.
- Eventually, since the methods in [7,8] cannot deal with the transients caused by capacitor discharge in fault voltage signals due to external fault conditions, these methods have failed in all cases. However, as can be seen in Table 13, the proposed method has successfully dealt with this condition.

From Tables 12 and 13, it should be noted that the inclusion of C&SFs 7–9 made the proposed method more complex compared to the state-of-the-art. However, the proposed method can deal with different challenges (i.e. the challenges in Table 12) of the element failure detection for various SCB configurations with promising accuracy and speed of convergence, compared with existing methods.

5 Conclusion

The inability of having fast condition monitoring of the capacitor units, may result in extensive damage to the SCBs. In this study, a new algorithm for online monitoring of the SCBs is proposed that focuses on finding the faulty phase and the number of failed capacitor units. Depending on the grounding systems of the SCBs, the proposed algorithm uses the fundamental component of the voltage or the current signal as an input parameter of the algorithm. The performance of the proposed algorithm was evaluated by different types of SCBs. By applying different types of fault scenarios for different types of SCBs, it can be concluded:

- The proposed method can be successfully used for capacitor unit failure detection in internally/externally fused and fuse-less configurations.
- The proposed method detects and calculates element failures within one cycle delay after a failure takes place.
- The decaying DC component leads to significantly large errors in the calculation of the fundamental component, which results in delayed decision making (i.e. more than one cycle delay.) The proposed method can deal with the decaying DC component due to external faults for protection of the SCBs; so that the decision making remains within almost one cycle.
- The proposed method can detect and calculate simultaneous element failures in different phases.

Simulation results also show that this algorithm can detect the element failures of SCBs, during simultaneous failures in multiple phases. As a result, it can be utilised for the protection of SCBs.

While the proposed method has provided notable accuracy and fast response compared to the state-of-the-art, it should be noted that due to phasor based calculation, the proposed method yet has one cycle delay in acquiring authenticated response. Therefore, more work should be done to reduce these time delays.

6 References

[1] Dhillon, M., Tziouvaras, D.: 'Protection of fuseless shunt capacitor banks using digital relays'. 26th Annual Western Protective Relay Conf., Spokane County, Washington, USA, October 1999

[2] '*Eaton's Cooper power systems catalog: power capacitors*' (Cooper Power Systems, Shanghai, China, July 2014)

[3] Agrawal, K.C.: '*Industrial power engineering and applications handbook*' (Butterworth-Heinemann, MA, USA, 2001)

[4] Bishop, M., Day, T., Chaudhary, A.: 'A primer on capacitor bank protection', *IEEE Trans. Ind. Appl.*, 2001, **37**, (4), pp. 1174–1179

[5] Price, E., Wolsey, R.: 'String current unbalance protection and faulted string identification for grounded-wye fuseless capacitor banks'. 65th Annual Georgia Tech Protective Relaying Conf., Atlanta, Georgia, USA, May 2011

[6] Zhang, M., Du, J., Chang, H., *et al.*: 'A shunt capacitor detection method based on intelligent substation'. 2017 IEEE Conf. on Energy Internet and Energy System Integration (EI2), Beijing, China, 2017

[7] Jouybari-Moghaddam, H., Sidhu, T., Voloh, I., *et al.*: 'New method of capacitors failure detection and location in shunt capacitor banks'. 2018 71st Annual Conf. for Protective Relay Engineers (CPRE), College Station, Texas, USA, 2018

[8] Jouybari-Moghaddam, H., Sidhu, T.S., Zadeh, M.R.D., *et al.*: 'Enhanced fault-location scheme for double wye shunt capacitor banks', *IEEE Trans. Power Deliv.*, 2016, **32**, (4), pp. 1872–1880

[9] Jouybari-Moghaddam, H., Sidhu, T.S., Zadeh, M.R., *et al.*: 'Enhanced fault location scheme for double wye shunt capacitor banks', *IEEE Trans. Power Deliv.*, 2017, **32**, (4), pp. 1872–1880

[10] Gajic, Z., Ibrahim, M., Wang, J.: 'Method and arrangement for an internal failure detection in a y-y connected capacitor bank'. US Patent 20 130 328 569, December 2013

[11] Ali, M.: 'Fault analysis and fault location in fuseless split-wye shunt capacitor banks'. 2019 Int. Symp. on Recent Advances in Electrical Engineering (RAEE), Islamabad, Pakistan, vol. 4, 2019

[12] Samineni, S., Labuschagne, C., Pope, J., *et al.*: 'Fault location in shunt capacitor banks'. 10th IET Int. Conf. on Developments in Power System Protection (DPSP 2010). Managing the Change, Manchester, UK, March 2010, pp. 1–5

[13] Schaefer, J., Samineni, S., Labuschagne, C., *et al.*: 'Minimizing capacitor bank outage time through fault location'. 2014 67th Annual Conf. for Protective Relay Engineers, College Station, Texas, USA, March 2014, pp. 72–83

[14] Samineni, S., Labuschagne, C., Pope, J.: 'Principles of shunt capacitor bank application and protection'. 2010 63rd Annual Conf. for Protective Relay Engineers, College Station, Texas, USA, March 2010, pp. 1–14

[15] Kasztenny, B., Schaefer, J., Clark, E.: 'Fundamentals of adaptive protection of large capacitor banks - accurate methods for canceling inherent bank unbalances'. 60th Annual Conf. for Protective Relay Engineers, 2007, College Station, Texas, USA, March 2007, pp. 126–157

[16] Kalyuzhny AMccall, J.C., Day, T.R.: 'Corrective device protection'. US Patent 7 973 537, July 2011

[17] Abedini, M., Davarpanah, M., Sepehr, A., *et al.*: 'Shunt capacitor bank: transient issues and analytical solutions', *Int. J. Electr. Power Energy Syst.*, 2020, **120**, p. 106025
[18] Machado, A.A.P., Antunes, H.M.A., Pires, I.A., *et al.*: 'Probabilistic assessment and evaluation of transients in a medium voltage three-phase capacitor bank energized by unsynchronized vacuum switchgears'. 2016 IEEE Industry Applications Society Annual Meeting, Portland, Oregon, USA, 2016, pp. 1–11
[19] Gumilar, L., Cahyani, D.E., Afandi, A.N., *et al.*: 'Optimalization harmonic shunt passive filter using detuned reactor and capacitor bank to improvement power quality in hybrid power plant'. AIP Conf. Proc., Solo, Indonesia, 2020, vol. 2217, no. 1, p. 030003
[20] De Araujo, L.R., Penido, D.R.R., Carneiro, Jr.S., *et al.*: 'Optimal unbalanced capacitor placement in distribution systems for voltage control and energy losses minimization', *Electr. Power Syst. Res.*, 2018, **154**, pp. 110–121
[21] Sadeghian, O., Oshnoei, A., Kheradmandi, M., *et al.*: 'Optimal placement of multi-period-based switched capacitor in radial distribution systems', *Comput. Electr. Eng.*, 2020, **82**, p. 106549
[22] Abdelsalam, A.A., Mansour, H.S.E.: 'Optimal allocation and hourly scheduling of capacitor banks using sine cosine algorithm for maximizing technical and economic benefits', *Electr. Power Compon. Syst.*, 2019, **47**, (11–12), pp. 1025–1039
[23] 'IEEE guide for the protection of shunt capacitor banks'. IEEE Std C37.99-2012 (Revision of IEEE Std C37.99-2000), March 2013, pp. 1–151
[24] 'C70 capacitor bank protection and control system'. UR Series Instruction Manual, GE Digital Energy, November 2014
[25] Sidhu, T.S., Zhang, X., Albasri, F., *et al.*: 'Discrete-Fourier-transform-based technique for removal of decaying DC offset from phasor estimates', *IEE Proc., Gener. Transm. Distrib.*, 2003, **150**, (6), pp. 745–752
[26] Ernst, T.: 'Fuseless capacitor bank protection'. Proc. Minnesota Power Systems Conf., Minnesota, USA, 1999, pp. 77–83